Determining Stellar Classes Using Spectroscopy

Michael Lowry

Advisor: Dr. David Gore

April 22, 2024

Contents

1 Abstract

This project investigates the relationship between the spectrum of a star and its temperature and classification. Stars can be described as black bodies which follow Planck's Law. Planck's Law describes the relationship between the spectrum of light emitted by a black body and its temperature. Additionally, the different stellar classes used by astronomers roughly follow a temperature scale, decreasing in temperature from class O to class M. The goal of this project was to classify several stars by recording their spectra, determining their black body or "effective" temperature using Planck's Law, and then classifying them based on this temperature.

I recorded spectra of the stars Sirius, Betelgeuse, Aldebaran, Alphard, Capella, and Pollux using the Star Analyser 200 diffraction grating, a telescope, and a monochrome CCD. I wavelength-calibrated and corrected each spectrum for instrument response using the RSpec spectrum analyser software. I then used simple Python code to correct the spectra for atmospheric reddening due to Rayleigh scattering and to fit a black body curve to each spectrum, from which I determined the effective temperature of each star. I then compared these temperatures to a temperature scale for stellar classification to determine the class of each star.

My results for Aldebaran, Alphard, Capella, and Pollux were within 15% of the actual values. Unfortunately, the spectrum peaks of Betelgeuse and Sirius were outside of my instrument's sensitivity range, resulting in very poor fits with large uncertainties. Therefore, I decided to focus on classifying the other four stars. I classified Aldebaran, Alphard, Capella, and Pollux to be K10, K7, F10, and G10 respectively, while their actual classifications are K5, K3, G8/G0, and K0. The determined classes for Aldebaran, Alphard, and Pollux are within five stellar subclasses of the actual classes. My determined class for the double star Capella is, at worst, nine subclasses outside the actual classification. These results are reasonable for the amateur equipment and software I used and the approximate nature of matching a star's temperature to its class. The temperatures and classes I found are also self-consistent with one another since they follow the same relative order as the reference values.

2 Introduction

Stars can be described as black bodies which follow Planck's Law. Planck's Law relates the temperature of a black body to its emitted spectrum of light. As temperature increases, the peak of the spectrum shifts from red to blue wavelengths. Fitting a spectrum to Planck's Law should return a temperature that matches with professional estimations of the star's temperature. Additionally, since the Harvard stellar classification scheme roughly follows changes in temperature, this temperature should be indicative of a star's spectral class.

This project used the Askar 103 APO triplet refractor telescope, Celestron AVX equatorial mount, Orion Starshoot G4 monochrome CCD camera, and the Star Analyser 200 diffraction grating to record spectra of Sirius, Betelgeuse, Aldebaran, Alphard, Capella, and Pollux for analysis. Uranus and the carbon star UU Aurigae were also recorded for their interesting spectra (see appendix). Additionally, I used the spectrum analyser software RSpec to view and calibrate the spectra. Finally, I coded a Python script to first correct the spectrum for atmospheric reddening and then fit the spectrum to a Planck curve to extract the temperature of the star. I matched this temperature to a range of temperatures corresponding to a stellar class and subclass.

The PCSE Department's Schmidt-Cassegrain telescope (SCT) was initially chosen due to its large aperture and lack of chromatic aberration, but I decided on using my own triplet refractor and equatorial mount since the equatorial mount was much better at tracking stars than the alt-az mount of the SCT. The triplet refractor corrects for chromatic aberration inherent to refractive optics to a large degree, but not completely.

The monochrome astronomical camera was the best choice for capturing spectra since it lacks the Bayer filter which decreases the sensitivity of the sensor to certain wavelengths of light. It also has a large sensor for capturing more of the spectrum. This camera was also already in the possession of the Department.

The Star Analyser 200 (SA 200) is a commercially available diffraction grating that attaches to the end of an astronomical camera. It has twice the diffractive capability of the Star Analyser 100 since it has twice as many lines per millimeter. It is capable of producing higher resolution spectra since the resolvance of a grating is proportional to the number of lines illuminated. Furthermore, it is significantly cheaper than higher resolution diffraction gratings. Overall, its ease of use and its capability to produce higher resolution spectra at a modest price point made it the go to choice for this project. Additionally, the same company responsible for the SA 200 created the companion software RSpec. This software is easy to use and has many built in tools that make calibrating and correcting spectra incredibly easy.

This setup was the most cost effective way to record spectra and calibrate them in order to fit them with a black body curve. While more expensive slit spectrometers would be able to obtain much higher resolution spectra, this would require additional expense and more exposure time to achieve a bright spectrum.

3 Theory

Planck's Radiation Law describes the spectral irradiance of a black body as

$$I = \frac{2\pi hc^2}{\lambda^5}\left[\frac{1}{e^{\frac{hc}{\lambda k_B T}} - 1}\right] \tag{1}$$

where h is Planck's constant, λ is the wavelength of light, c is the speed of light, k_B is Boltzmann's Constant, and T is the temperature of the black body [1]. Since the spectra intensity recorded will be in arbitrary units, this equation can be modified by a constant scaling factor for purposes of fitting to data:

$$I = A\frac{2\pi hc^2}{\lambda^5}\left[\frac{1}{e^{\frac{hc}{\lambda k_B T}} - 1}\right] \tag{2}$$

In this form, the equation becomes a two parameter fit for A and T, with the latter being the effective temperature determined by the spectrum.

Before a spectrum can be fitted it must be wavelength calibrated and corrected for instrument response. Calibration involves telling RSpec where different spectral lines are in the image, after which it does a fit to determine the wavelength values of the rest of the pixels. Instrument response correction adjusts the the spectrum for variations in sensitivity to different wavelengths of light by the sensor. This first requires finding the instrument response curve of the system given by the following equation

$$R(\lambda) = \frac{I_{sys}(\lambda)}{I(\lambda)} \tag{3}$$

where R is the instrument response curve of the system, I_{sys} is the spectrum captured by the system, and I is the actual spectrum [2]. R for a setup can be found by dividing a spectrum recorded using the specific system by a professionally corrected spectrum which represents the actual spectrum profile of the star, many of which are available in RSpec. After the instrument response curve for a particular system is found, any spectrum captured with that system can be corrected by simply dividing it by the instrument response curve.

As the light of a star travels through the earth's atmosphere, some of the blue light is lost because of Rayleigh scattering. The strength of this effect increases as the star appears closer to the horizon since the star's light has to travel through more of the atmosphere before being collected by the telescope. The following equation describes the ratio between the spectrum of the star before and after Rayleigh scattering

$$\frac{I(\lambda,\infty)}{I(\lambda,r_1)} = \exp\left[\frac{r_0}{e^{r_1/r_0}}\frac{32\pi^3}{3N_0}\frac{1}{\lambda^4}\left(A + \frac{B}{\lambda^2} + \frac{C}{\lambda^4}\right)^2\right] \tag{4}$$

where $I(\lambda, \infty)$ is the spectrum of the star before hitting the atmosphere, $I(\lambda, r_1)$ is the spectrum collected by the telescope, r_1 is the height of the observation site above sea level, r_0 is the scale height of the atmosphere, 7640 meters, divided by the cosine of the zenith angle of the star, A, B, and C are the Cauchy constants at standard temperature and pressure, and N_0 is the number density of particles at sea level [2]. As the zenith angle decreases and wavelength increases, the ratio approaches one. By rearranging the equation, an experimental spectrum can be corrected for Rayleigh scattering by multiplying it by this ratio.

4 Methods

4.1 Data Acquisition

Before capturing spectra, I assembled and aligned the equatorial mount to the North celestial pole. I set the tripod as level as possible facing towards geographic north. I then aligned the mount using five stars. The hand controller of the mount chose several stars to align to, slewing to each one to be centered in the eyepiece. After the alignment is completed, I slewed the telescope to my target star using the mount's GoTo function and inserted the camera with the SA 200 attached to it. I used a 3D printed adapter to screw the SA 200 inside a 1.25" spacer which I attached to the end of the camera to achieve my desired spacing between the SA 200 and the CCD sensor (Figure 1).

Figure 1: SA 200 attached to camera via adapter and 1.25" spacer

I found the brighter, blazed spectrum by looping captures and slewing the scope, then centered it in the frame. It is best to have the star a fair bit away from the side of the frame to make stacking less difficult later on. Autostakkert!, the program I used to stack the captures to reduce noise, uses user defined alignment points to ensure features in the frames are combined correctly. If the star is to close to the edge of the frame, it is not possible to use it as an alignment point, which makes it impossible to get good results when stacking. It is possible to loop image capture to make this step easier. With my setup, the star appeared to the right of the brighter spectrum. I then chose the exposure duration with decent brightness by performing several test captures.

I evaluated the spectrum focus by eye and tried to maintain a crisp and bright image. I found that that best focus was achieved when moving the telescope's focuser to around

13mm or 11mm as indicated by markings on my telescope's focusing tube. While I did try to use the focusing tool in RSpec, I found it a little difficult to work with since there was no direct connection between RSpec and the camera. Instead, the software had to automatically open the images as they were saved to a particular folder. The tool did help, but once I saw what a focused spectrum looked like, I could discern good focus without using it.

After focusing, I captured over 20 frames of the star at my chosen exposure time. I then repeated the process for any other stars I decided to capture that night. Finally, I put the cap on the end of my telescope and recorded 20 plus dark frames for each exposure time I recorded at that night.

4.2 Calibration

Before the spectrum can be processed, I had to figure out how to convert from pixels to wavelengths in the spectrum. I did this by collecting the spectrum of a hydrogen vapor tube in the same manner as I did for stars, minus alignment. I put the tube outside McMurran and set up the telescope in front of Christopher Newport Hall. I did this using the SCT since I initially planned to use it instead of my telescope, but the spectrum still worked for my later setup since I did not change the spacing of the SA 200.

Once captured, the gas spectrum was loaded into RSpec. Knowing the emission lines of hydrogen, I completed wavelength calibration and saved the calibration settings (cf. tutorial video 20 [3]). After I did this, I was able to calibrate any other spectrum taken with the same setup using One Point Calibration; all RSpec needs to know is where the 0th order spectrum, or star, is.

4.3 Processing

Before stacking the images, I subtracted the dark images using Planetary Imaging PreProcessor (PIPP), an astronomical image processing software. Then, I loaded the new images into the astronomical stacking software Autostakkert! and, using the Surface mode, analysed the frames and then placed alignment points on the star. I made sure the range is set to 14 bit. Otherwise, the program may misrepresent the image.

If the spectrum was slightly dim, I opened the stacked image in GIMP and adjusted the levels to brighten the image. After opening this file in RSpec, I converted pixels to wavelengths using One Point Calibration with the previously created calibration setting file (cf. tutorial video 24 [3]). I then checked the calibration by overlaying different spectral lines and seeing how they line up with features in the spectrum.

After I calibrated the spectrum, I corrected it for instrument response (cf. tutorial video 15 [3]). I used Sirius to create the instrument response curve since it is extremely bright. I loaded a reference spectrum for an A0V star, smoothed it, and then divided the experimental

spectrum by it, as shown in equation (3). After some final smoothing, I ended up with an instrument response curve. All I had to do after this was divide my calibrated spectra by this curve to get corrected spectra. After making some annotations to point out relevant absorption features, I saved the spectrum profile and synthesised color spectrum as a png file.

To correct for atmospheric reddening and get the temperature of the star, I read in the final spectrum as a data frame with corresponding wavelengths and intensities into my Python script. The script first corrected for atmospheric reddening by multiplying the spectrum by the ratio in equation (4). It calculated this ratio using the zenith angle at the time of capture. Afterwards, it ran a fit using equation (2). For my initial guesses for the parameters A and T, I used the maximum intensity of the spectrum and the actual temperature of the star, respectively. After fitting, my script saved an image of the fit alongside the input spectrum as well as a table containing the fitted temperature, its standard deviation, and the percent error between it and the actual temperature.

To classify the star, I divided each stellar class into 10 equivalent "buckets" of temperature ranges corresponding to each subclass and matched the fitted temperature to a bucket. While this is not really how stars are classified, it does give an idea of how my methods have done in classifying a star. The Cannon or Harvard scheme for stellar classification is based on relative absorption features, but it does follow a general trend in temperature.

5 Data

Below are the final annotated spectra of Sirius, Capella, Pollux, Alphard, Aldebaran, and Betelgeuse, in order of decreasing temperature. The horizontal axis is in nanometers while the vertical axis is in arbitrary units of brightness. As is expected, the younger, hotter Sirius has elemental lines corresponding to hydrogen while the rest, being dimmer and older stars, have absorption features of heavier elements. Additionally, as the temperature of a star decreases, its peak wavelength of emission is noticeably shifted to the red end of the spectrum.

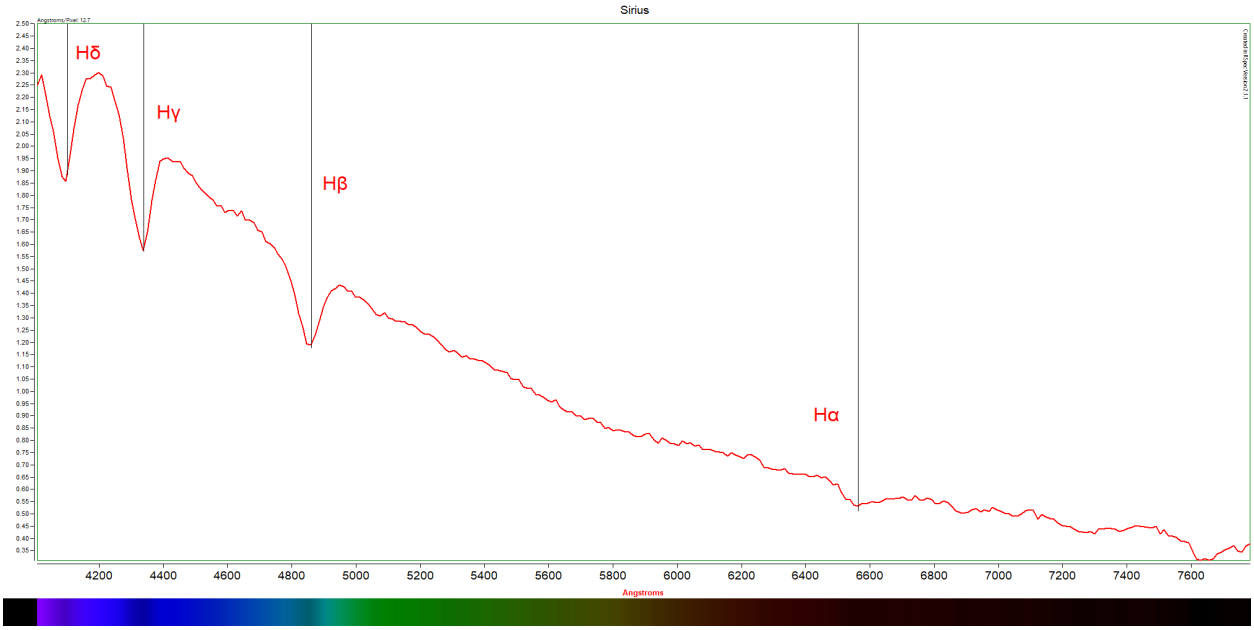

Figure 2: Spectrum of Sirius

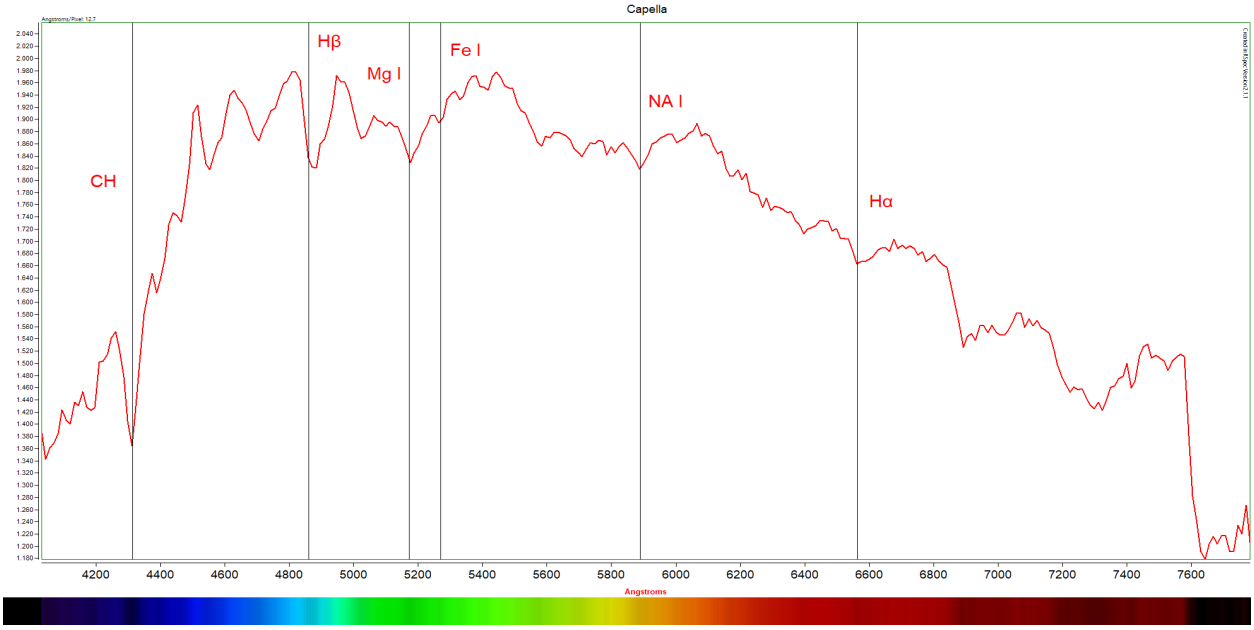

Figure 3: Spectrum of Capella

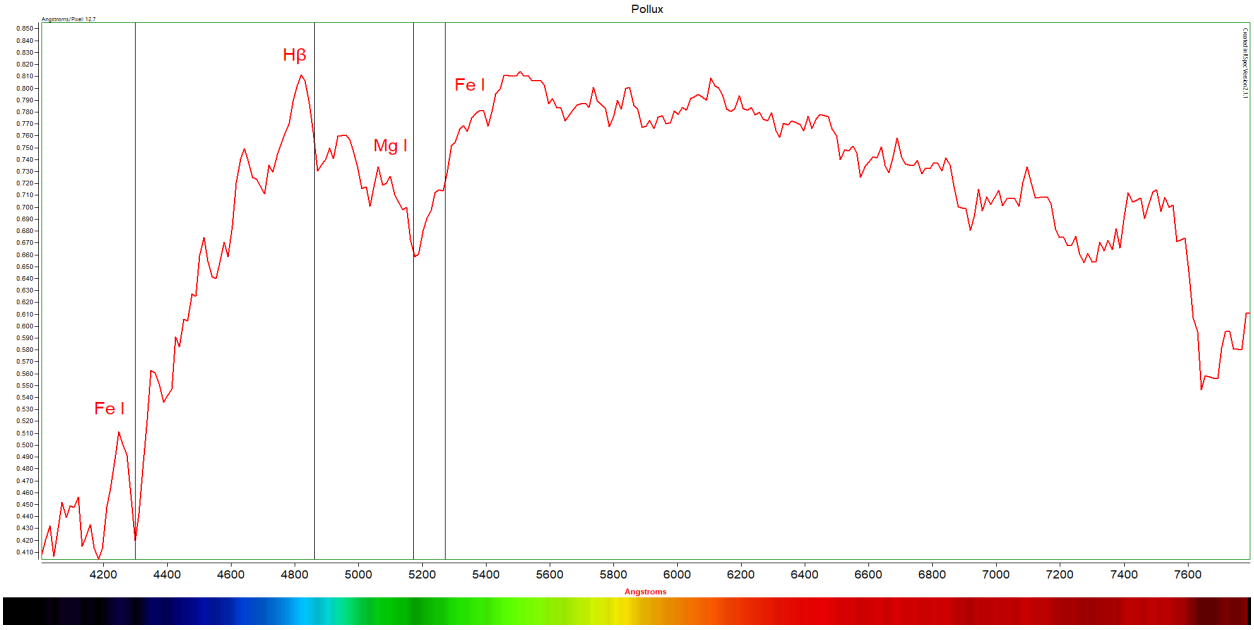

Figure 4: Spectrum of Pollux

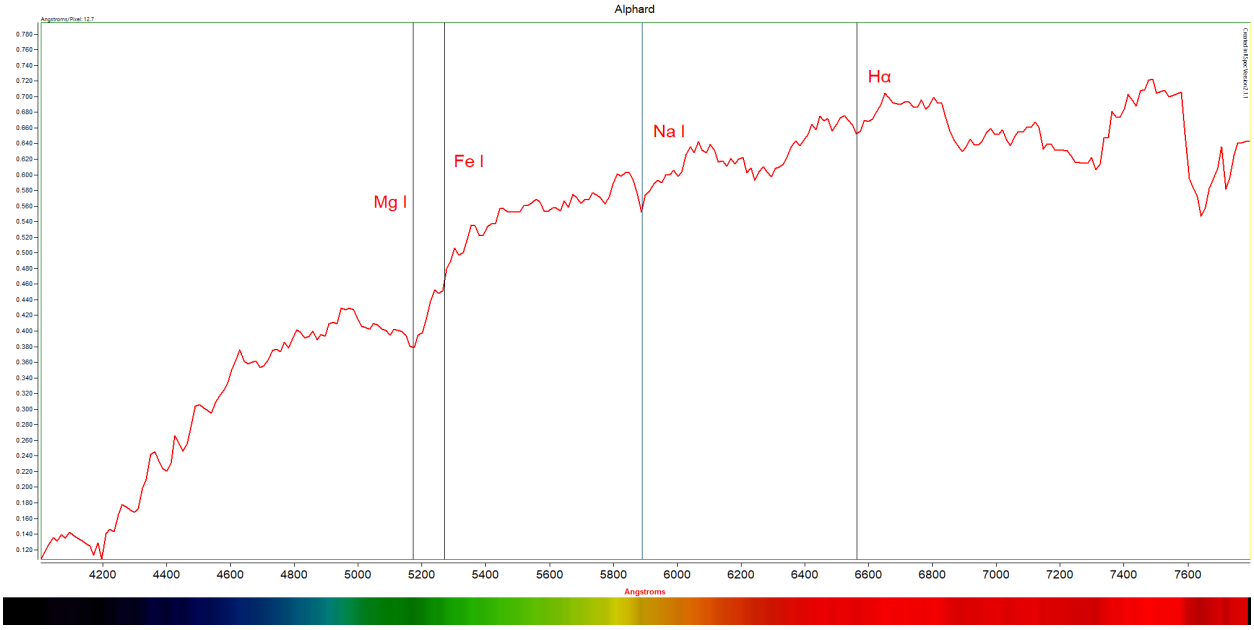

Figure 5: Spectrum of Alphard

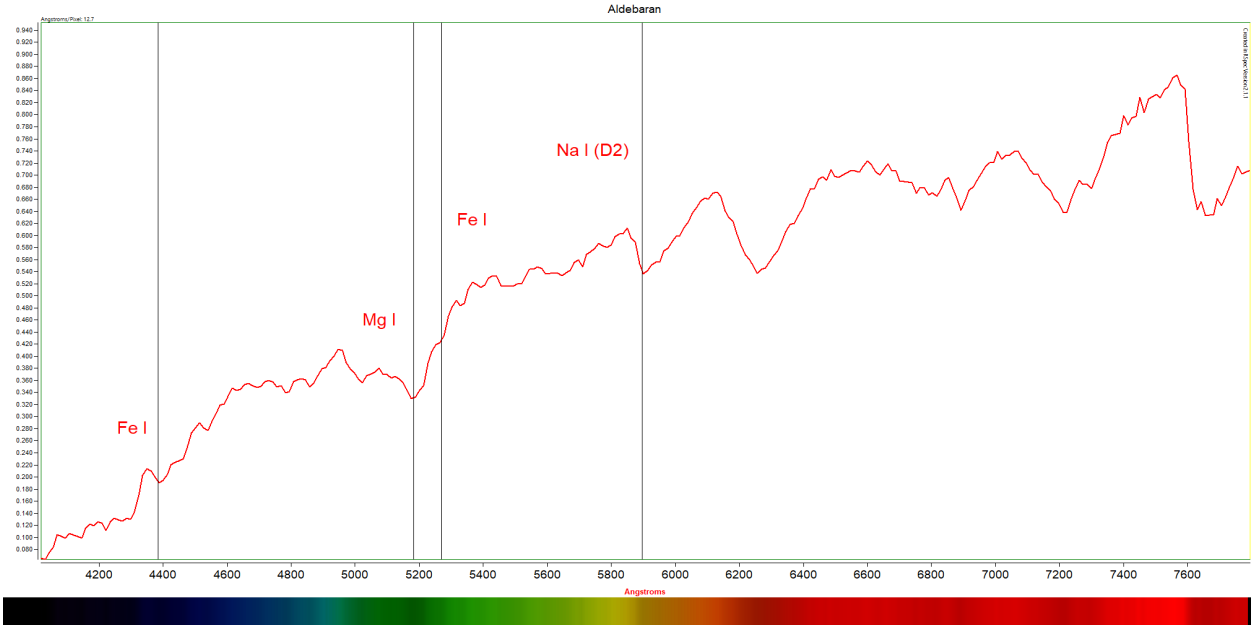

Figure 6: Spectrum of Aldebaran

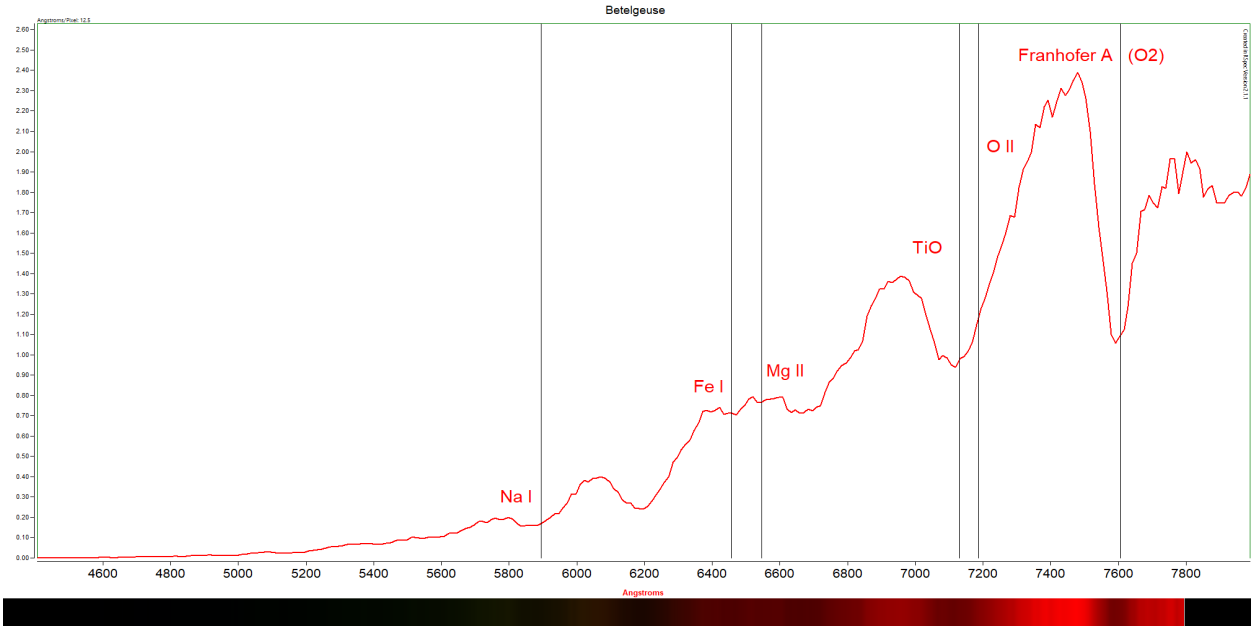

Figure 7: Spectrum of Betelgeuse

Table 1 includes the results of the black body curve fit for each star before and after correction for atmospheric reddening correction. The classes were determined using the experimental temperature after atmospheric reddening correction. Except for Sirius and Betelgeuse, the experimentally determined temperature agrees well with the actual value. The temperatures of Aldebaran, Alphard, Capella, and Pollux are within 12% of the reference values before correction and within 15% after correction. The experimentally determined classes are also within reason for the equipment used, lying at most eight subclasses within the actual class. A number is added to indicate subclasses, with a 10 being the coolest type of that class and 0 being the hottest. Additionally, the temperatures and classes are self-consistent, following the same relative order as the reference values. There is a general decrease in temperature in the Harvard classification scheme of OBAFGKM, in order. No class was determined for Betelgeuse or Sirius since their fits were visibly incorrect (see appendix).

Star	$\boldsymbol{T(\times 10^3 K)}$	$\boldsymbol{T_1(\times 10^3 K)}$	$\boldsymbol{E_1}$	$\boldsymbol{T_2(\times 10^3 K)}$	$\boldsymbol{E_2}$	**Class**	$\boldsymbol{T_2}$ **Class**
Aldebaran	4.010	3.56(2)	-11.27	3.75(2)	-6.37	K5	K10
Alphard	4.260	3.80(2)	-10.72	4.15(2)	-2.59	K3	K7
Capella	5.300∗	5.45(2)	2.90	6.06(2)	14.32	G8, G0	F10
Pollux	4.770	4.87(2)	2.18	5.27(2)	10.51	K0	G10
Betelgeuse	3.650	1.90(3)	-47.89	1.90(3)	-47.31	M1	NA
Sirius	9.880	14.2(2)	43.51	60(7)	503.89	A1	NA

Table 1: Results of black body fit and classification. T_1, E_1 are the temperature and percent error found before atmospheric reddening correction while T_2, E_2 are the temperature and percent error from the corrected spectrum. The reference temperature of Capella used is an average of the temperatures of Capella Aa and Capella Ab.

6 Discussion and Conclusion

Before correction for atmospheric reddening, the black body fit temperatures for Aldebaran and Alphard were within 12% of the actual temperatures, while the experimentally determined values for Pollux and Capella were within 3% of the actual effective temperatures. After correction, the experimental temperature for Aldebaran jumped to roughly 6% under the actual value while the fit temperature of Alphard improved to just 2% under the actual temperature. The fits for the corrected spectra of Capella and Pollux overestimated the temperature of each by 14% and 10% respectively. Unfortunately, none of these temperatures are within one standard deviation of the actual value. It was also not possible to achieve reasonable temperatures for Sirius and Betelgeuse, likely due to the fact that the sensitivity range of my equipment clipped the emission peak of both stars, resulting in a very difficult fit.

In general, the correction for Rayleigh scattering resulted in improved values for the stars for which the initial fits underestimated the temperature while doing the opposite for stars whose temperatures were initially overestimated. This is to be expected since the correction effectively shifts the peak of the spectrum to the blue end, resulting in a higher experimental temperature. Additionally, it shifts the peak of the cooler stars less than the hotter stars since it adds more signal to blue wavelengths of light, resulting in greater movement for peaks which are towards the blue end of the spectrum. One explanation for the larger percent error for the hotter stars is random error when capturing and processing the spectra. It could also be due to improper focus across the spectrum since the triplet optics of the telescope do not completely remove chromatic aberration. Therefore, part of the spectrum could be in crisp focus while the other is not, leading to a deviation from theory for a star that peaks in the part of the spectrum that is unfocused. Taking this into account, the experimentally acquired temperatures are well within reason for the amateur equipment used.

The experimentally determined stellar classes are also reasonably close to the actual classes. The experimentally found classes of Aldebaran and Alphard are within five subclasses of their actual class. The F10 class found for Capella is above the G0 and G8 classifications of the binary stars that make it up by one and nine subclasses respectively. The experimentally determined class G10 is larger than the actual class K0 for Pollux by one subclass. The discrepancies in the classification comes from the fact that there is no strict equivalence between a class and a star's temperature and the corresponding error in the experimentally found temperatures. These determined classes are well in line with the actual classes considering the corresponding errors in temperature and variations arising from classifying a star in this unintended manner. Additionally, the order of these experimentally determined temperatures and classes are consistent with the order of the actual temperatures and classes of the stars analysed.

Overall, the results in effective temperature and classification of Aldebaran, Alphard,

Capella, and Pollux are reasonably close to their actual values when taking into account uncertainties arising from amateur equipment and classifying solely off of temperature. Unfortunately, it was impossible to get usable results for Sirius and Betelgeuse since the peak of their spectra lay outside the sensitive range of the camera. However, by looking at the spectra of each star that was recorded, it is easy to see that there is a direct correlation between a star's temperature and the peak of their spectrum, as is described by Planck's Law. Therefore, this project was successful in determining the effective temperature and classification of four stars, while also illustrating Planck's Law.

7 Appendix

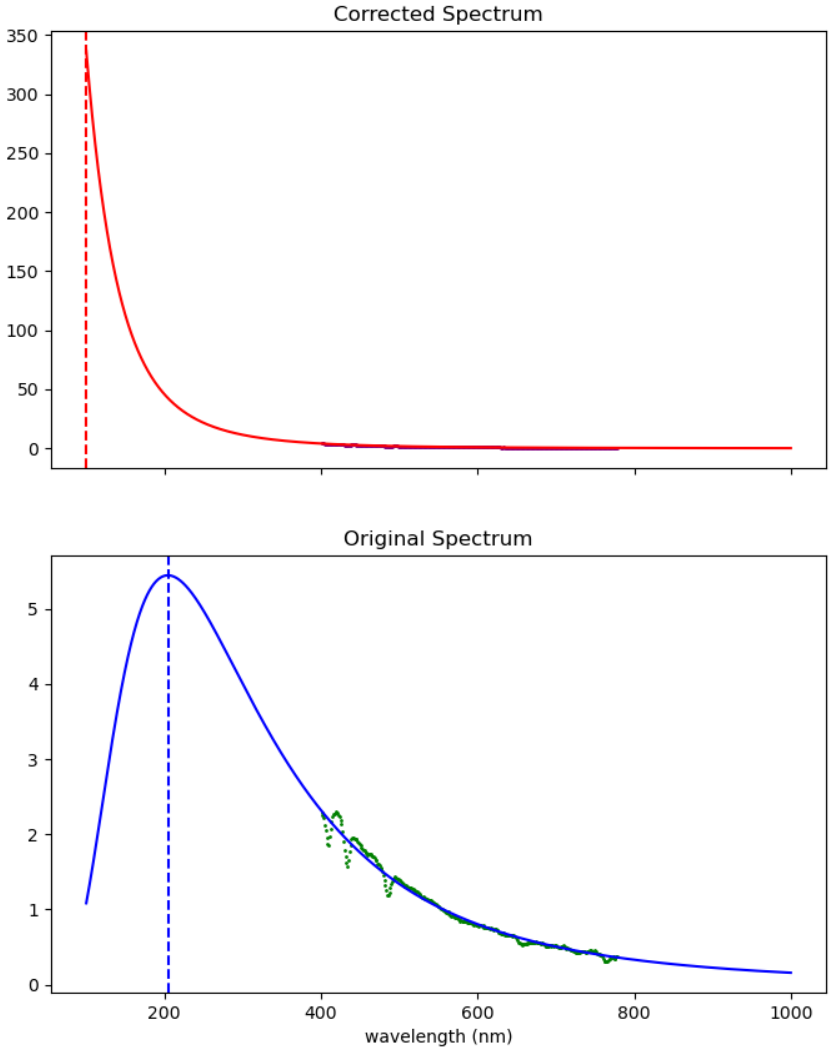

Figure 8: Fit of Sirius

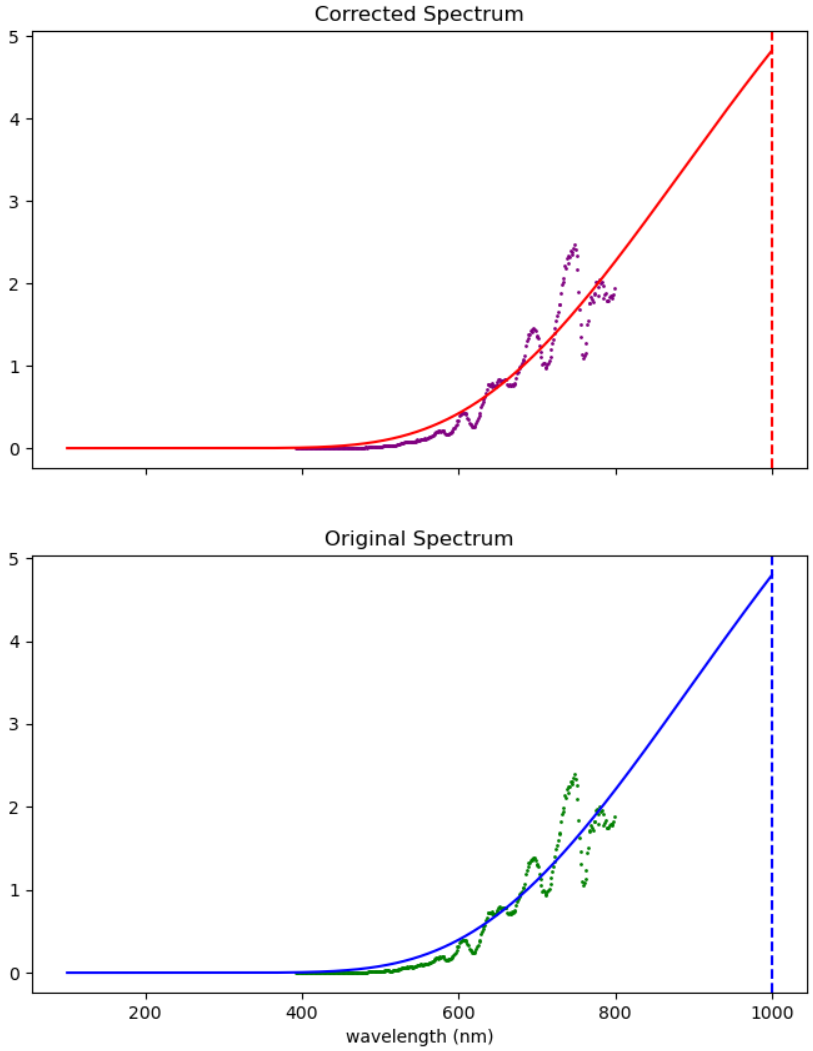

Figure 9: Fit of Betelgeuse

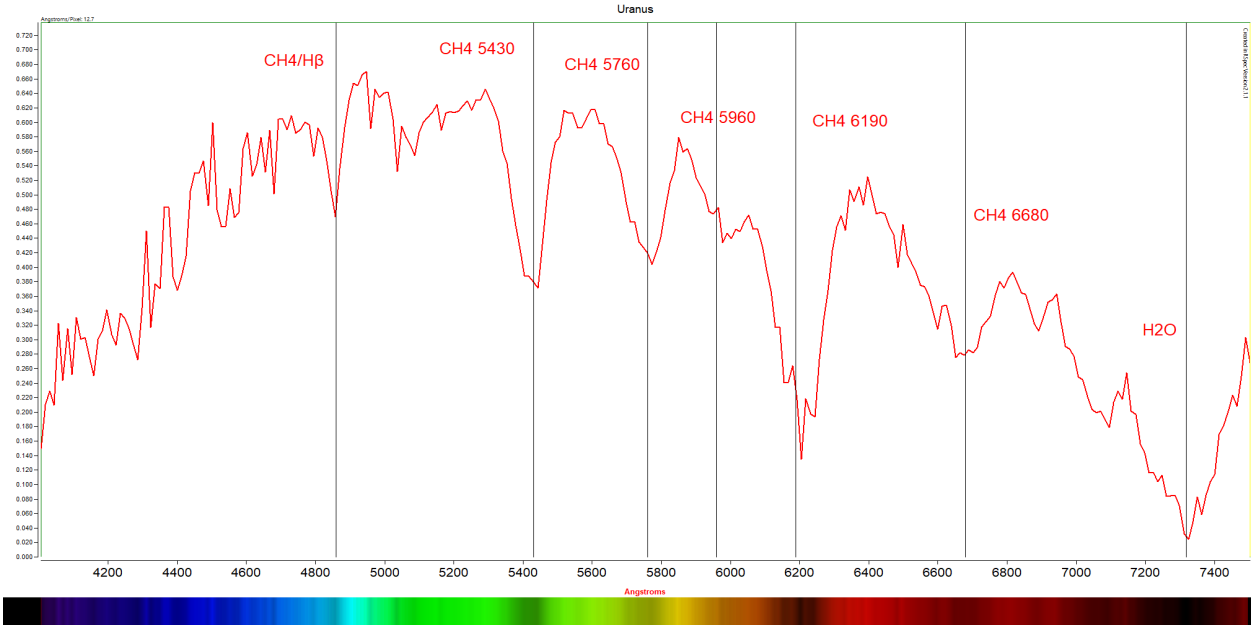

Figure 10: Spectrum of Uranus. Notice absorption bands from methane and water in its atmosphere.

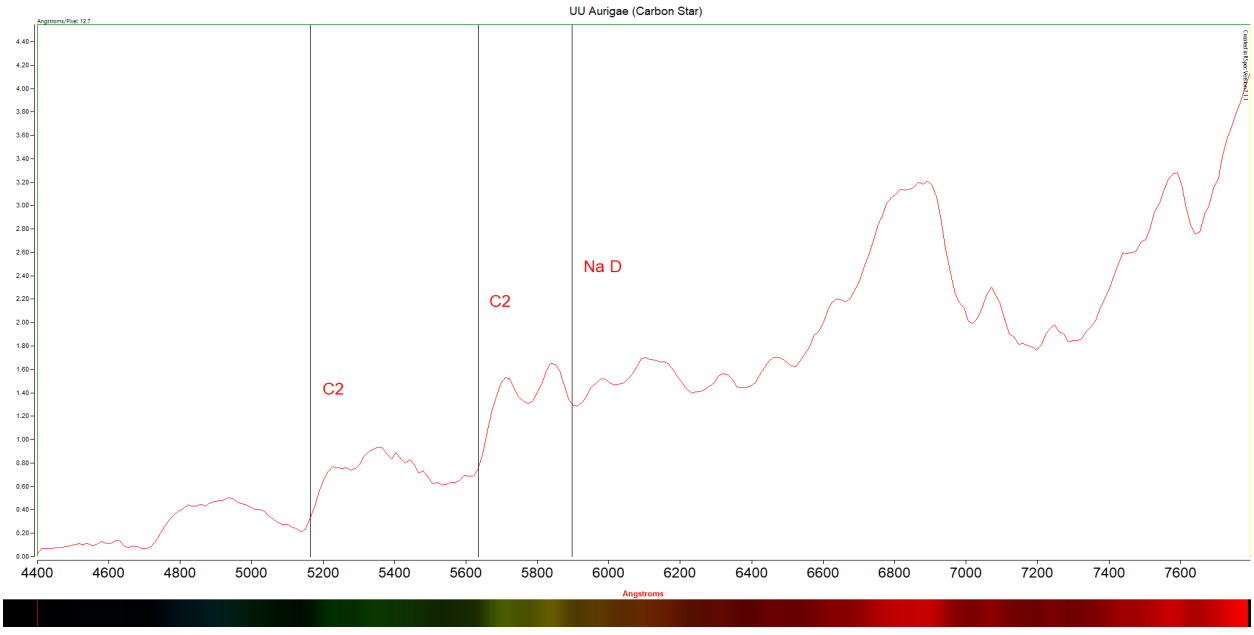

Figure 11: Spectrum of UU Aurigae. As a carbon star, it is abundant in diatomic carbon.

8 Resources

[1]E. Hecht, *Optics*, 2nd edition (Addison-Wesley, 1990).

[2]D. Cenadelli, M. Potenza, and M. Zeni, "Stellar temperatures by wien's law: not so simple", Am. J. Phys. **80**, 391–398 (2012).

[3]*Rspec videos*, `https://www.rspec-astro.com/more-videos/`.